Flexible Test and Demonstration Vehicle Platform for Electric Drivetrain Power Electronics

C. Sültrop
Friedrich-Alexander-University Erlangen-Nuremberg
Chair of Electron Devices
Erlangen, Germany
Email: christian.sueltrop@leb.eei.uni-erlangen.de

F. Hilpert, M. Giegerich, M. Wenger, M. März
Fraunhofer Institute for
Integrated Systems and Device Technology IISB
Erlangen, Germany
Email: florian.hilpert@iisb.fraunhofer.de

***Abstract*—This paper presents the design and implementation of an experimental electric vehicle platform. The platform is intended for demonstrating and testing highly integrated power electronics drivetrain components in an actual vehicle, rather than just in laboratory and test bed environments. Most of these components were created in earlier research projects. The high voltage network topology is flexible enough to incorporate future developments and additional power electronics systems. A central vehicle control unit routes the signal flow between the vehicle's electronic control units. It also controls the interaction of the drivetrain power electronics systems. Adding and exchanging devices is supported by the modular design of the vehicle control unit software. Special attention is given to the battery system, which was purposely designed for the vehicle platform.**

***Index Terms*—power electronics, electric vehicle conversion, electric vehicle, BEV, drivetrain, powertrain, vehicle control unit, BMS, battery system**

I. Introduction

Full or partly electrification of the vehicle drivetrain as in hybrid electric vehicles (HEV), plug-in hybrid electric vehicles (PHEV), and battery electric vehicles (BEV) is seen as a contribution to the goal of global and local reduction of CO_2 and other emissions created by individual traffic. Modern power electronics systems are considered a key technology to contribute to that goal, as they permit efficient conversion between electrical voltage levels and wave forms at high power. They can transfer high amounts of energy in short time between electrical energy sources, storages, and sinks.

Current research goals include improving power density and electromagnetic compatibility (EMC) of drive systems [1] and mechanical and functional integration of power electronics with motors and battery systems [2]. Increased user convenience during the battery charging process is expected from inductive charging technology [3], while DC charging [4] and DC grid integration [5], [6] promise reduced charging times and integration of electric vehicles into the prospected smart electricity grid.

Power electronics research projects typically focus on a narrowly defined research objective. When technology demonstrators are created, maturity in terms of functions, safety features, interfaces, communication protocol specifications, and documentation is often not a main objective. Thus, maturity in these fields is reduced compared to state-of-the-art solutions. The same applies for test coverage and reliability, raising the hurdles for vehicle integration.

Nevertheless, practical experience with the performance of the technology created, in terms of user experience and interoperation of different vehicle power electronics systems, can only be collected if the systems are integrated into a real vehicle. Thus, an internal combustion engine (ICE) vehicle was converted into a BEV. For both the drivetrain power electronics systems and the auxiliary power electronics systems, technology demonstrators were used exclusively. The resulting test platform is designed to be flexible in two main regards: First, regarding issues arising from the aforementioned special characteristics of the technology demonstrators built in. Second, regarding the integration of future developments.

Besides the testing aspect, the vehicle created is also meant to draw attention to electric vehicle technology. The vast majority of potential vehicle buyers regards electric vehicles as environmental friendly and rational. Qualities like sportiness, good looks, and driving pleasure effect buying decisions on an emotional level, but are not associated with electric vehicles by a majority of potential vehicle buyers [7]. Thus, a sports car was selected for conversion to contradict this common view.

II. General Design Considerations

To attenuate the aforementioned maturity issues of technology demonstrators, one project goal was to gain maximum flexibility regarding the availability of auxiliary devices and to limit possible interference between devices that have not been operating together before. The goal was addressed by the following measures:

1) Implementation of a modular vehicle control unit (VCU) using model based rapid prototyping software and hardware. The VCU routes and manages all communication between devices.
2) Splitting the VCU software into modules that are version controlled individually to adopt to the special needs of test stand, integration, and final operational phases of the individual units and the completed vehicle.
3) Implementing of different HV current paths for driving mode and charging mode that can be enabled separately to preclude mutual interference.

4) Options to bypass devices and to exclude functions that are not vital, not mature, or increase system complexity on both hardware and software level. Thus, these issues can be addressed in a divide-and-conquer manner, and additional features can be added as the system stability increases.
5) Easy and quick access to the drivetrain components to simplify maintenance.

The following sections describe how these objectives are addressed by the vehicle architecture, especially by the newly designed battery system, and by the modular VCU software.

III. Vehicle Architecture

The donor vehicle is an Artega GT sports car that was previously propelled by an internal combustion engine (ICE) located in the rear of the vehicle. The converted vehicle is depicted in Fig. 1. The ICE and the auxiliary devices such as gear box and gas tank were removed. The rear of the vehicle is constructed as a steel framework bolted on an aluminium space frame that forms the cockpit and the front partition. Thus, necessary modifications to fit in the electric drive unit and the battery system into the former ICE installation space were possible at reasonable expense.

Figure 1. Converted vehicle performing track tests.

The majority of devices integrated in the test and demonstration vehicle are technology demonstrators developed at Fraunhofer IISB in different earlier research projects.

An overview of the packaging, the high voltage (HV) network, and the coolant circuits of the test platform vehicle is shown in Fig. 2. Two highly integrated units located in the rear of the vehicle are the key elements of the electric drivetrain. First, the battery system (drawn green), which consists of eight battery modules with cell monitoring, a battery management system (BMS), a conductive charging unit, and two sets of junction contactors. The battery system is discussed in more detail in Section IV.

Second, a twin-drive unit (drawn orange), which propells each rear wheel individually. The unit is further described in Section III-A.

Two different coolant circuits were implemented: a battery circuit and a motor circuit, as described in Section III-D.

A multi port DCDC converter and the VCU are located inside the (dashed) passenger cabin, behind the seats. A DCDC converter supplying the 14 V power network and the cabin heating systems are located in the front. Two seperate coolant

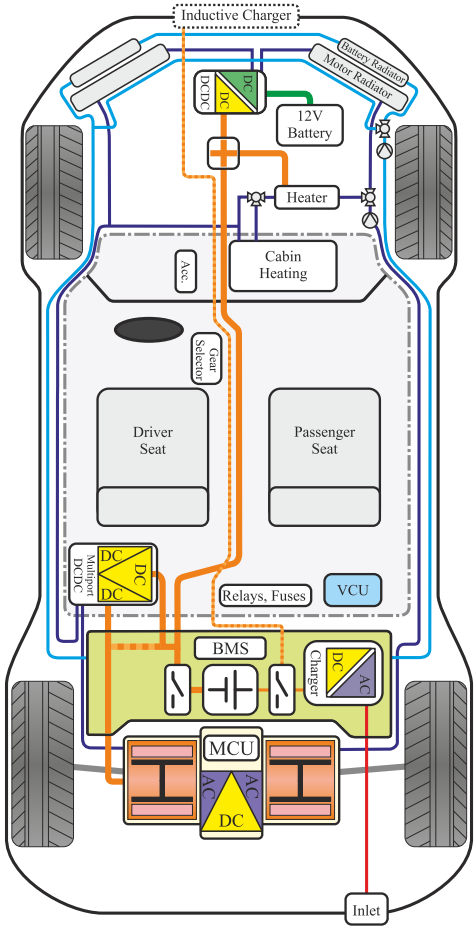

Figure 2. Topology of the realized vehicle. Low voltage power network and signal buses are omitted for reasons of clarity.

circuits (dark/light blue) exchange heat between the power electronics systems and the radiators. The DC HV network (orange) runs between the battery and the drive unit and connects the auxiliary systems. Due to separate contactors, the charger sub-net can be connected to the battery stack independently from the main circuit.

A. Drive Unit

The twin-drive unit integrates two mechanically independent three-phase permanent magnet synchronous machines (PMSM), two sets of gears, two drive inverters sharing a common distributed dc-link capacitor, and the motor control unit (MCU) in a single, liquid cooled case. The drive inverters are constructed from six *Inverter Building Blocks* (IBB), each of which combines an IGBT commutator cell, a gate driver, a dc-link capacitor, and a current sensor on a single replaceable module [8], see Fig. 3. As motors and inverters are integrated in one common case, HV wiring is reduced to a short DC connection between drive unit and traction battery. The motors' mechanical independence, in conjunction with the individual control of both motors by the MCU, offers two simplifications compared to a single motor design: First, axle drive and differential are obsolete; second, torque

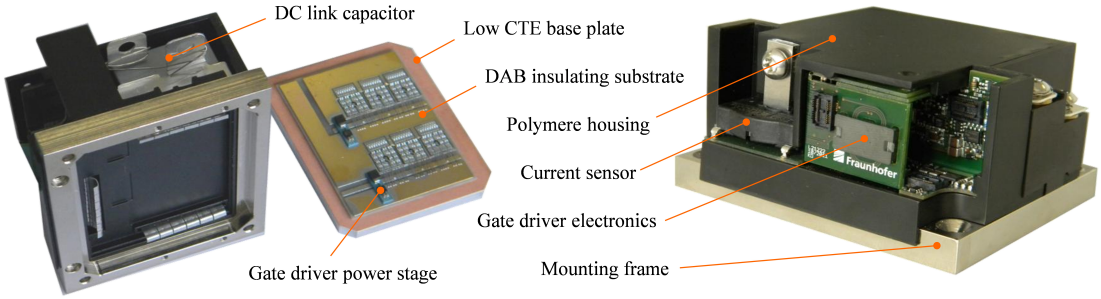

Figure 3. Inverter Building Block [8].

Table I
INTEGRATED DRIVE UNIT TECHNICAL DATA

Parameter	Value
construction	PMSM
maximum power	2 × 80 kW
maximum motor torque	2 × 230 Nm
maximum motor speed	10,000 RPM
transmission factor	7:1
weight	170 kg
controller	field oriented control
electrical interface	high voltage DC
communication interface	CAN

vectoring can be implemented in software, without additional mechanical parts. The drive unit is placed between the rear wheels, with a modest offset to the rear and connected to the wheels by axle shafts.

Technical data of the drive unit is given in Table I and an image is shown in Fig. 4.

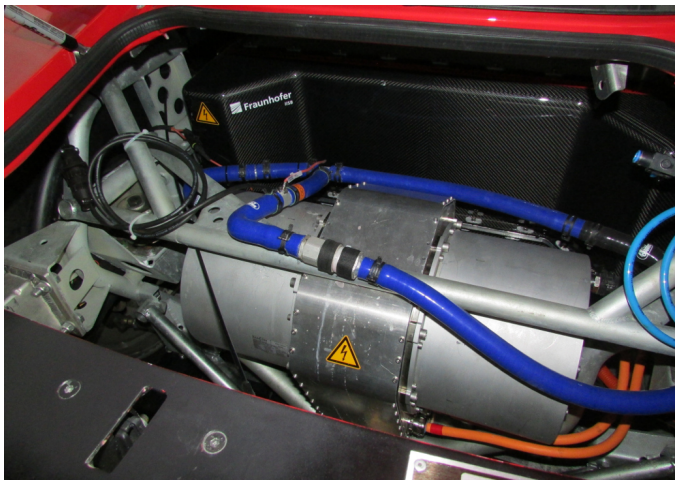

Figure 4. Twin PMSM drive unit located between the rear wheels, seen through the tailgate. Behind it is the smart battery system in a black carbon-fibre composite (CFC) case.

B. Power Electronics Systems

In addition to the drive unit and the battery system described in Section IV, a number of other power electronics systems was integrated in the vehicle.

First, a uni-directional high voltage to low voltage (HVLV) DCDC converter is mounted in the vehicle front. It converts from the HV traction battery voltage level to the 14 V low voltage (LV) network level and supplies power to the drivetrain ECUs, sensors, and actuators, as well as to the original vehicle LV network. A 120 Ah deep-cycle tolerant absorbent glass mat lead-acid (AGM) battery serves as a fall-back power supply if the HVLV converter is not available, thus increasing the vehicle's tolerance to faults of this critical device.

Second, a multi port bi-directional HV DCDC converter transfers energy and shifts voltage levels between the traction battery and two other devices. One port can provide variable voltage to the drive inverter dc-link capacitors, independent from the actual battery voltage. The IGBT traction inverter efficiency depends on the dc-link voltage, as does the beginning of the field weakening range of the PMSM machines. Thus, shifting the dc-link voltage can increase the overall system efficiency [9]. The other port can be used to implement high voltage DC charging, to add an inductive charger [3], or to add a second energy storage based on battery, super-capacitor, or fuel cell technology. For reducing dependency on the HV DCDC converter and for assessing system behavior with the traction battery directly connected to the dc-link, it can be bypassed in the battery system.

Third, a one-phase 3.7 kW on-board charger was derived from the modular charger described in [10]. It connects the vehicle to the 230 V AC grid and creates DC voltage for charging the traction battery. The charger consists of an ACDC front-end connected to the AC grid and an isolated DCDC backend that provides galvanic isolation and is connected to the vehicle's HV network. Adjusting the dc-link voltage to the battery voltage permits operating the charger at a high efficiency of more than 94 percent over nearly the whole operation range. A Type 2 charging inlet at the vehicle rear is provided for connecting the charger to a charging station.

Fourth, a third-party off-the-shelf 6 kW positive temperature coefficient (PTC) heater is integrated into the drive unit coolant

circuit and connected to the HV network, as further described in Section III-D.

C. E/E-Networks

The electrical and communication networks interconnect the vehicle components and transport electrical energy and communication signals. Energy is transferred within the HV networks at 320 V to 380 V – depending on the battery's depth of discharge (DoD) –, and in a traditional 14 V low voltage (LV) network. Signals are primarily transferred on Controller Area Network (CAN) busses, but PWM, analog, and digital signals exist as well.

The LV power networks and signal networks are two-part: New networks were created in parallel to the original vehicle networks, which have been left intact. The original power network and the new LV network are connected at the AGM battery. The VCU routes between the original drivetrain CAN bus and the newly integrated CAN busses. In the following, only the new networks are discussed.

1) HV Energy Network: The HV network is depicted in Fig. 2. A major partition of the network is implemented inside the battery system. Eight battery modules are connected in series. A service disconnect cuts both battery poles from the HV network during maintenance, making sure no voltage can be applied to the battery system interface sockets. The network is divided in two sub-networks which can be activated separately by the BMS via contactors: The traction path is connected to the battery system's interface sockets, while the charging path is connected to the conductive charger internally, permitting driving and charging of the vehicle to be addressed separately, precluding mutual interference. This measure also ensures that operating the motors is impossible during charging, regardless of actions taken by the VCU software.

The HV networks are secured by an interlock line that opens all contactors if an HV plug is disconnected or if the emergency stop button in the cockpit is pressed.

2) LV Network: The DCDC converter depicted in Fig. 5 transfers energy from the HV network to the 14 V LV network. During charging, the LV network can also be supplied by an ACDC converter that accompanies the HV charger.

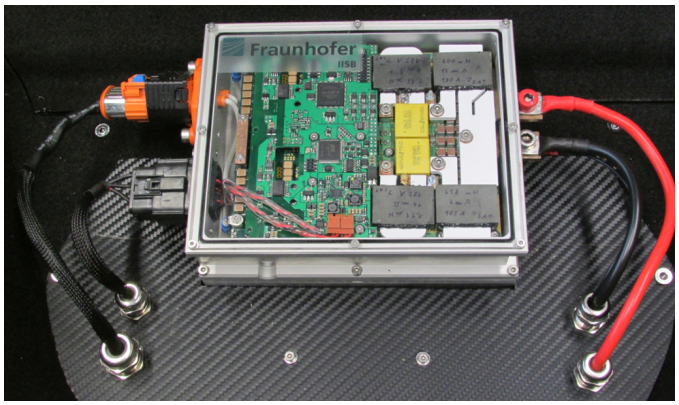

Figure 5. A DCDC converter that transfers energy from the HV network to the LV network is located in the vehicle front compartment.

3) Signal Network: The ECUs and power electronics systems are connected with each other and with the VCU in different signal networks, as depicted in Fig. 6. The ECUs that were added to the vehicle are connected to the main CAN bus. The MCU, which controls the integrated drive system, is connected to a destinct bus. Thus, it is impossible for other units to disturb the communication link between MCU and VCU. Whereas the ECUs are physically connected to the same bus, all communication is logically routed through the VCU; ECUs do not communicate directly. Thus, all higher level functionality that involves more than one unit is located in the VCU.

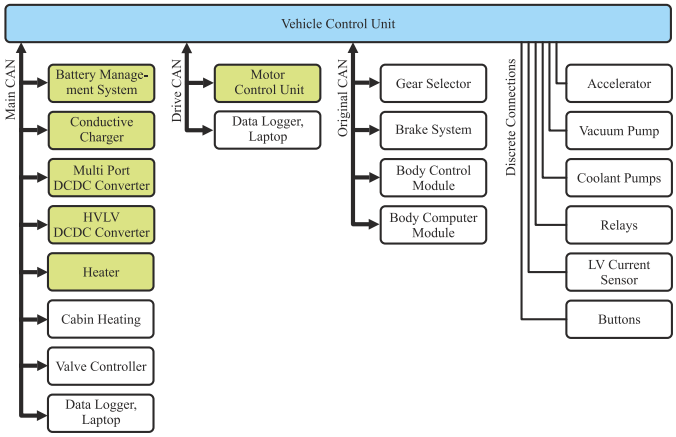

Figure 6. The signal network consists of CAN busses and discrete connections. Power electronics systems are drawn green.

The VCU is also connected to the original drivetrain CAN bus and exchanges data with some of the remaining original ECUs. This includes gear selector position, wheel speeds measured by the brake system, or brake light activation requests during recuperation.

Some auxiliary systems are connected to the VCU via discrete connections, such as PWM, analog, and digital signals.

D. Coolant Circuits

The coolant circuit re-uses the original radiators of the combustion engine and the air conditioning system. An ECU controls the valves and collects temperature measurement data at different points in the circuit for experiments and temperature control. As depicted in Fig. 2, two distinct coolant circuits were implemented.

First, the drive unit coolant circuit connects the drive unit with the former combustion engine radiators in the front. The radiators can be bypassed through the PTC heater and optionally through the cabin heat exchanger. The effects of using the drive unit thermal masses to store heat energy for cabin heating during charging were evaluated in [11].

Second, the battery system is connected to the former air condition radiators.

The radiators can be bypassed in order to heat the battery system with its own conduction losses. The cooling concept for the battery is described further in Section IV.

Table II
VEHICLE MASS DISTRIBUTION

Parameter	Value Before Conversion	Value After Conversion
vehicle empty mass	1245 kg	1325 kg
axle load (front)	535 kg (43 %)	458 kg (43.3 %) without battery and driver
axle load (rear)	710 kg (57 %)	600 kg (56.7 %) without battery and driver
side load (left)	N/A	537 kg (50.7 %) without battery and driver
side load (right)	N/A	521 kg (49.3 %) without battery and driver

E. Mass Distribution

Table II states the vehicle mass and mass distribution before and after conversion of the vehicle. Vehicle mass after conversion is close to the mass before conversion. Axle load distribution, and thus the center of gravity, is expected to be shifted to the rear with the battery mounted. Vehicle dynamics are therefore expected to be more rear-biased than in the original vehicle. With 537 kg and 521 kg the side loads are practically identical after conversion.

IV. BATTERY SYSTEM

Both the mechanical construction and the BMS electronics and software of the smart battery system are designed for meeting the demands of a highly modular vehicle test platform.

A. Construction

The mechanical structure consists of two parts: An aluminium supporting structure for carrying the main load, and carbon fibre composite (CFC) covers for taking over shear forces. The supporting structure realizes a functional integration of carrying and cooling. It consists of three friction stir welded aluminium cooling plates (drawn blue in Fig. 7). They divide the battery compartment in an upper and lower section and provide double sided cooling to the eight individual battery modules. The cooling plates can be interconnected in different configurations for cooling strategy investigations. Leakage free fluid connectors on the cooling plates are positioned outside the battery case. Thus, the design realizes a complex but lightweight fluid cooled system without fluid gaskets inside the sealed battery compartment. EMC shielding is integrated into the CFC covers, which are shown in Fig. 8.

The BMS is integrated in the upper compartment, together with an optional HVLV DCDC converter. The lower compartment comprises the junction box with contactors, service disconnect, isolation monitoring and a switching mode power supply to accommodate the LV network during charging. Finally, the ACDC battery charging system is integrated at the bottom side of the lower cooling plate, using the battery system cooling circuit.

The battery system is inserted and mounted to the vehicle body from below. The service disconnect and the electrical

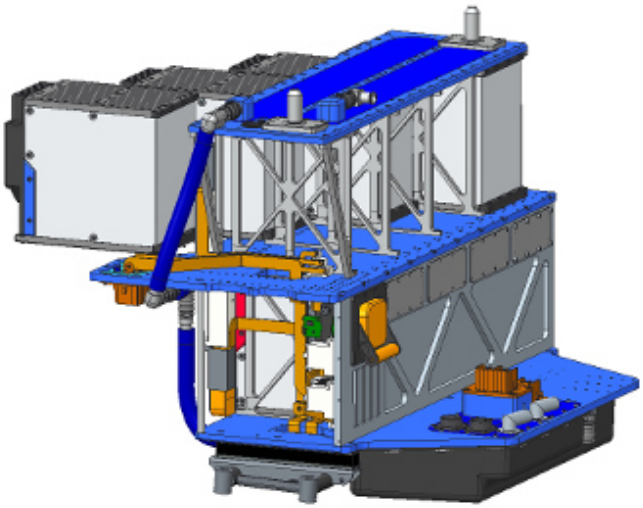

Figure 7. CAD drawing of the battery system supporting structure. Battery module insertion is illustrated for the upper compartment.

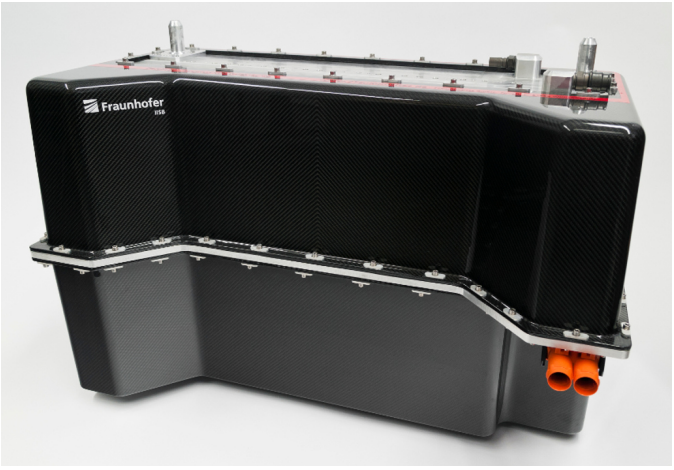

Figure 8. The battery sytem is contained in a CFC case. The drive unit is connected via the DC plug on the lower right side. The system is connected to the vehicle's coolant circuit via the fluid connectors on each cooling plate. The spines on top guide and secure the system when inserted into the vehicle from below.

connections located to the front right in Fig. 7 can be accessed from the passenger cabin as shown in Fig. 10. In total, the external electrical interfaces can be summarized as follows:

- 3x HV traction connectors for e.g. drivetrain, HV DCDC converter and DC charging
- 2x HV low power connectors for HV auxiliary components like e.g. HVLV DCDC converter and inductive charging system
- 1x connector to the Mode 2 charging socket at the vehicle rear
- 1x combined connector for 14 V supply and CAN communication
- 1x 63 pole signal connector to route various signals to the VCU if desired and providing programming interfaces to BMS and charger ECUs

Table III
BATTERY SYSTEM TECHNICAL DATA

Parameter	Value
cell type	KOKAM SLPB100216216H
cell chemistry	Lithium-Ion Nickel Manganese Cobalt Oxide (LiNMC)
cell construction	prismatic pouch
no. of battery modules	8
no. of cells per module	12
battery nominal capacity	13.6 kWh
min/nom/max battery voltage	259/355/403 V
min/max cell voltage	2.7/4.2 V
min/nom/max current	-120/320/480 A
cell internal resistance	< 0.8 mΩ
system weight	195 kg
no. of traction/charge path external ports	3/1
charger interface	Mode 2
communication interface	CAN
balancing	passive
coolant medium	mix of glycol and water

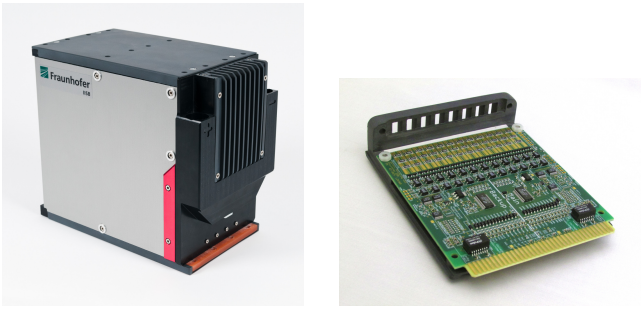

(a) Battery module. (b) Monitoring board.

Figure 9. Each of the eight battery modules contains twelve pouch cells and a monitoring circuit board.

The battery system technical data is stated in Table III.

B. Battery Modules

Each of the eight battery modules depicted in Fig. 9 (a) contains twelve Lithium-Ion Nickel Manganese Cobalt Oxide (LiNMC) pouch cells and a monitoring circuit board. The cells are connected in series by ultrasonic welding and mounted on floating cooling plates. The housing is machined from an ultralight aluminium sandwich material. The two thermal contact surfaces expand to their respective top and bottom cooling plates, while being electrically isolated from the battery container via thermally conductive plastic plates.

In order to ensure safe and efficient operation of the battery system, every single cell voltage, as well as the temperature inside the battery system, has to be monitored. Battery monitoring systems are commonly based on circuits using commercially available monitoring ICs. These ICs comprise integrated analog to digital converters (ADCs) to sense the battery cell voltages and temperatures. Besides providing a communication interface to the higher level BMS, these ICs are often also capable of controlling a cell balancing circuit.

The battery modules are specially designed to facilitate the integration and evaluation of different monitoring systems. The battery sense contacts for voltage measurement and the negative temperature coefficient (NTC) sensors for temperature measurement are all routed to a single wire-to-edge-card connector. A monitoring circuit board shown in Fig. 9 (b) with the according edge pattern can be directly accommodated by this connector and no additional contacting and wiring effort is necessary. For easy access, the monitoring printed circuit board (PCB) is mounted to the lid of the module, which is made of thermally conductive plastic. The lid is designed to act as a heat sink to dissipate the heat generated at the balancing resistors in case a passive balancing scheme is used. The monitoring circuits are connected in a daisy chain starting at the BMS in order to exchange measurement data and command messages. In the current implementation the communication is based on a galavanically isolated differential bus, which increases the robustness against electromagnetic interference.

C. Battery Management System

The BMS, which is mandatory to maintain the safe operation of the battery system, is realised as an embedded system platform. The stackable PCBs of this platform enable a highly modular and easily adaptable configuration of the BMS electronics. The system hardware is build from four interconnected PCBs:

- Microcontroller Platform Board
- System Basis Addon Board
- Application Specific Addon Board
- Daisy-chain Communication Interface Mezzanine Board

This structure enables adaptable configuration of the boards if, for example, the IC for the cell measurements is changed. The *Microcontroller Platform Board* comprises the microcontroller (INFINEON TRICORE automotive microcontroller) with its peripheral components, e.g. RAM and ROM, reset logic and clock devices. The *System Basis Addon Board* has the function to supply the other BMS electronics with an isolated power supply. A safety controller is also located on this board to monitor operation of the microcontroller. The isolated communication interface is implemented with CAN transceivers and isolator ICs. Application specific functionalities like relay and contactor control for main and charger lines, interlock feedback etc. are implemented on an application specific board. This board also hosts a mezzanine board, which adapts the BMS' serial peripheral interface (SPI) to the galvanically isolated daisy chain communication of the battery monitoring boards.

The embedded software of the BMS is based on the AUTOSAR automotive software framework. It abstracts the high performance microcontroller and its complex internal peripherals to a maintainable software complexity level. Thus, new algorithms such as battery state estimation and charging control can be implemented with reasonable effort.

V. Vehicle Control Unit

The vehicle control unit (VCU) is the central control and monitoring instance of the vehicle. It is programmed in MATLAB/SIMULINK/STATEFLOW and executed on a DSPACE MICROAUTOBOX II (MAB) rapid prototyping ECU. The MAB supplies CAN interfaces for connecting the VCU to the communication networks, plus digital and analog interfaces to connect with actuators and sensors like pumps, relays, buttons, or lamps.

The VCU communicates with other ECUs primarily on CAN. Primitive systems e.g. pumps, relays, buttons, or lamps are interfaced by either analog, digital, or PWM signals.

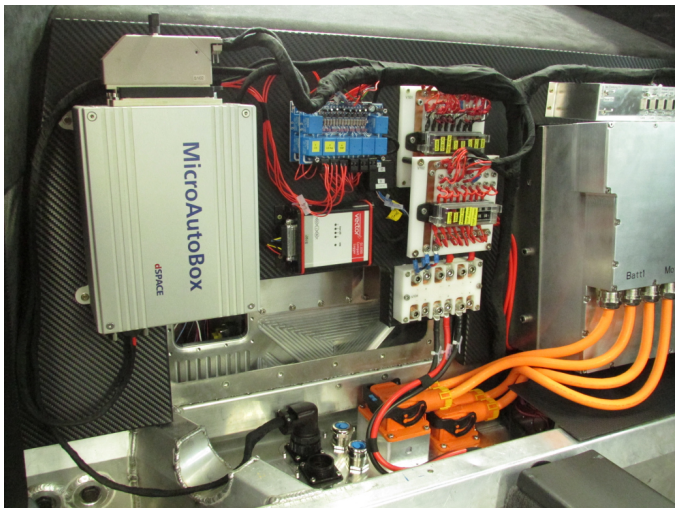

Figure 10. Vehicle control unit (left), relay boards, data logger, fuse boxes, power distributor (center), and multi-port DCDC converter (right) located behind the passenger seats. The battery connectors (bottom) are accessible from the cabin.

A. VCU Software Structure

The VCU serves three major tasks: First, control the operation of the sub-ordinate units. Second, simplify the units' complex interfaces for the higher level control software. Third, control vehicle operation by processing measurement data and state information received from the sub-ordinate units and by sending state requests and set values to those units. All communication between units is controlled by the VCU. State machines control the operation of the vehicle, according to the mode of operation selected by the driver.

The basic VCU software structure is illustrated in Fig. 11. The VCU software can be divided in three levels: Hardware abstraction layer, low level and high level.

The hardware abstraction layer (HAL) on the lowest level abstracts from the MAB hardware and is provided by the rapid prototyping ECU hardware supplier. It provides a Simulink block set to access the MAB CAN bus, analog, and digital I/O interfaces.

The next level, termed *low level* in Fig. 11, implements component driver modules for the drivetrain ECUs and other

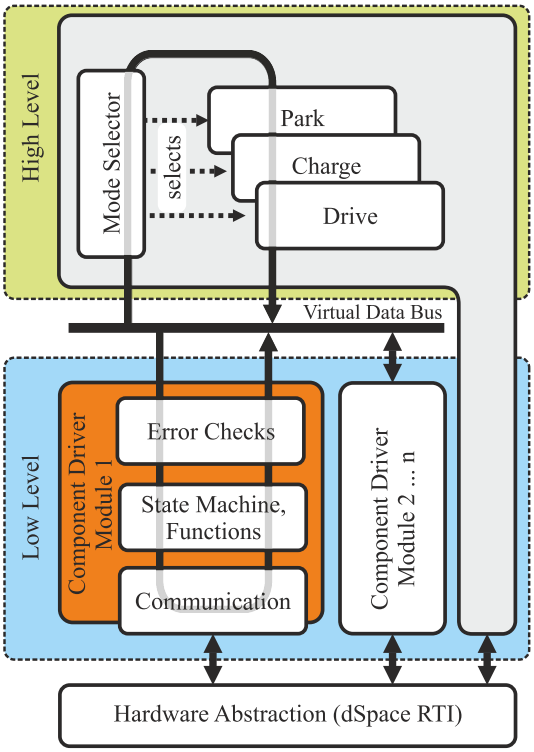

Figure 11. Basic VCU software structure.

units. The modules serve several goals: First, ECUs of technology demonstrators often have complex, not explicitly defined communication protocols. The driver modules implement these protocols and provide a simplified interface for the *high level* VCU software. Second, additional functions not (yet) implemented in an ECU can be created in the VCU as SIMULINK blocks instead. For simple systems that do not have an ECU, all software functions are implemented in the driver module. Each driver module has a state machine that ensures that the driver module is always in a defined state. Third, module level safe operation areas (SOA) prevent violating the specified operational bounderies of the respective systems.

The actual vehicle control software is implemented on the *high level*. The basic vehicle operating modes park, charge, and drive are implemented separately from each other. Based on driver input, a mode is selected by the *mode selector*. The *high level* software is connected to the component driver modules on the *low level* by a virtual data bus, which transports the input and output signals to and from the component driver modules.

B. Vehicle Operation

The high level software implements the basic functions expected from a BEV. This includes driving in forward and reverse direction, recuperation controlled by accelerator pedal position, speed limitation in both driving directions, and charging the vehicle at a charging station.

According to the selected mode of operation, the main and auxiliary system control units are booted and set up. In drive

Table IV
EXAMPLARY SOA IMPLEMENTATIONS

Objective	Measure
Ensure battery is operated in temperature SOA defined by cell manufacturer	De-rate maximum and minimum battery current based on cell temperature
Ensure battery cannot be over- or under-charged	Limit battery current as a function of battery SoC or voltage
Prevent de-magnatization of rare earth permanent magnets	Limit motor torque as a function of coil and capacitor temperatures
Reduce mechanical jerk between motor shaft and gearset	Limit torque request gradient
Prevent vehicle from driving reverse during recuperation	De-rate recuperation torque if wheel speed is below 5 km/h

mode, the driver sends request to the VCU via the gear selector and the accelerator. The requests are interpreted as system controller state requests and motor torque demands. The driver requests stimulate a state machine that controls the underlying component modules. The accelerator signal is interpreted as either a positive or negative torque request to the motors, depending on driving direction, accelerator position, and vehicle speed. Torque request generation takes into account possible power limits set by any of the drivetrain component modules, which can de-rate the battery current, converter current, motor torque etc. in order to fence safe operation areas (SOA) defined for the individual systems and the vehicle in whole. The ECU modules communicate dynamically updated maximum and minimum power constraints to the high level VCU software, which, in simple terms, limits the motor torque to make sure all power limitations are met. Examples of implemented SOAs are given in Table IV.

VI. EXPERIMENTAL RESULTS

Extensive experiments were performed on a roller dynanometer and verified on a test track to ensure the functional capability of the created test vehicle. A data logger can record all communication on the CAN bus, permitting detailed analysis of the system state variations. The plots discussed in this section examplariliy show data recorded from the vehicle CAN busses during a short test ride.

The bottom plot in Fig. 12 shows the accelerator position in percent. The upper plot shows the resulting torques generated by the left and right motors, as estimated by the motor controller. It can be seen that the generated torque is positive and follows the accelerator position as long as the position is above 30 %. When the accelerator position drops to zero at time t = 22 s, the generated torque becomes negative and goes up to zero as the vehicle approaches stand-still, see Fig. 13.

The accelerator characteristic is two-part: Below 30 %, negative torque is requested from the motors for recuperation, above 30 % positive torque is requested for acceleration. Between a vehicle speed of 0 km/h and 5 km/h, the negative torque request is multiplied with a factor between 0 and 1, proportional to the speed. Thus, negative torque is gradually

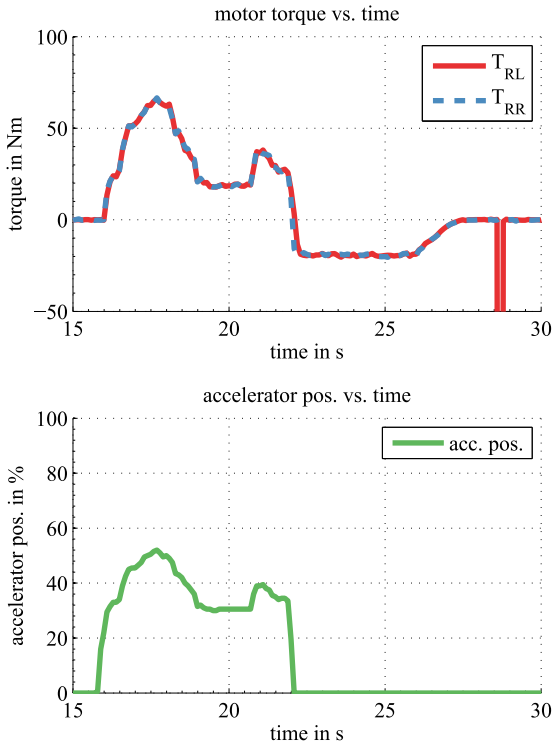

Figure 12. Accelerator position (bottom) and rear left and rear right motor torques (top).

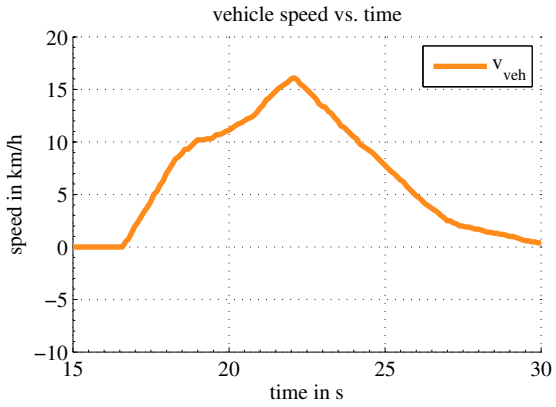

Figure 13. Vehicle speed measured by the brake system wheel speed sensors.

reduced to zero in the low speed area. This effectively prevents the vehicle from turning reverse after braking to stand-still due to negative wheel torque.

Fig. 13 depicts the vehicle speed measured by the original vehicle wheel speed sensors, resulting from the acceleration created by the motor torques applied to the rear wheels. The upper plot in Fig. 14 depicts the battery current measured by the BMS. When the torque is positive, current counted positive flows from the battery to the drive inverters' dc-link capacitors. When the generated torque is negative, the battery current is also counted negative. In the recuperation phase the motor torques are constant between t = 22 s and t = 26 s, while the

battery current is reduced proportionally to speed reduction. Both the highest and lowest individual battery cell voltages shown in Fig. 14 (bottom) decrease as the battery current increases and increase as the battery current decreases, due to the internal cell resistances.

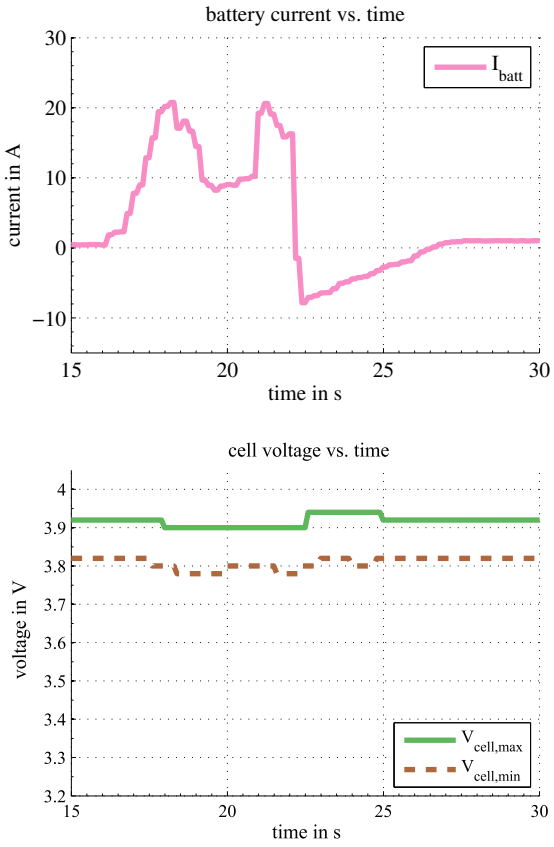

Figure 14. Battery current (top) and maximum and minimum cell voltages (bottom).

VII. Conclusions

The experimental results show that the implemented demonstration and test platform with its underlying hardware and software design is well-suited to create a fully functional vehicle. This is achieved by interconnecting technology demonstrators of drivetrain power electronics systems and auxiliary devices on both electrical and signal levels and adding high level vehicle control functions.

Flexibility to append additional devices and to exchange existing devices is provided on hardware level by the design of the HV network and the modularity of the battery system. On part of the VCU, the modularity of the implemented software concept strongly supports adding and modifying software functions, both in the higher level vehicle controller and the lower level ECU interface modules. Furthermore, the concept allows for a simplified initial start-up process of new power electronics systems and the creation of experiment specific software configurations.

The vehicle created will be approved for road service and thus will be used for testing current and future components and their interaction in real traffic situations, in addition to dynanometer and test track experiments.

References

[1] "Fortschrittsbericht 2014 – Bilanz der Marktvorbereitung," Nationale Plattform Elektromobilität, Berlin, Tech. Rep., Dec. 2014. [Online]. Available: http://www.bmub.bund.de/fileadmin/Daten_BMU/Download_PDF/Verkehr/emob_fortschrifttsbericht_2014_bf.pdf

[2] M. März, A. Schletz, B. Eckardt, S. Egelkraut, and H. Rauh, "Power electronics system integration for electric and hybrid vehicles," in *Proc. Integrated Power Electronics Systems (CIPS), 6th International Conference on*, Mar. 2010.

[3] C. Joffe, S. Ditze, and A. Rosskopf, "A novel positioning tolerant inductive power transfer system," in *Proc. Electric Drives Production Conference (EDPC), 3rd International*, Oct. 2013, pp. 1–7.

[4] D. Aggeler, F. Canales, H. Zelaya, D. L. Parra, A. Coccia, N. Butcher, and O. Apeldoorn, "Ultra-fast DC-charge infrastructures for EV-mobility and future smart grids." IEEE, Oct. 2010, pp. 1–8.

[5] A. Ipakchi and F. Albuyeh, "Grid of the future," *IEEE Power and Energy Magazine*, vol. 7, no. 2, pp. 52–62, Mar. 2009.

[6] W. Su, H. Eichi, W. Zeng, and M.-Y. Chow, "A Survey on the Electrification of Transportation in a Smart Grid Environment," *IEEE Transactions on Industrial Informatics*, vol. 8, no. 1, pp. 1–10, Feb. 2012.

[7] "Continental Mobilitätsstudie 2015: Präsentation der Ergebnisse," Jan. 2015. [Online]. Available: http://www.continental-corporation.com/www/download/presseportal_com_de/themen/initiativen/ov_mobilitaetsstudien_de/ov_mobilitaetsstudie2015_de/download_channel/mobistud2015_praesentation_de.pdf

[8] M. Hofmann, A. Schletz, K. Domes, M. März, and L. Frey, "Modular inverter power electronic for intelligent e-drives," in *Proc. Electric Drives Production Conference (EDPC), 2nd International*, Oct. 2012.

[9] M. Hofmann, B. Eckardt, M. März, and L. Frey, "Effizienzoptimierung integrierter elektrischer Antriebssysteme für Hybrid- und Elektrofahrzeuge," Aschaffenburg, 2010.

[10] J. Schmenger, S. Endres, S. Zeltner, and M. Marz, "A 22 kW on-board charger for automotive applications based on a modular design." IEEE, Oct. 2014, pp. 1–6.

[11] H. Rauh, M. März, L. Frey, and C. Sültrop, "Energy optimized implementation of climatisation systems in electric vehicles with integrated drive components," in *Conference on the Future of Automotive Technology*, Munich, 2014.